JOC Article

^{77}Se NMR Chemical Shifts of 9-(Arylselanyl)triptycenes: New Standard for Planar Structures of ArSeR and Applications to Determine the Structures in Solutions

Takashi Nakamoto, Satoko Hayashi, and Waro Nakanishi*

Department of Material Science and Chemistry, Faculty of Systems Engineering, Wakayama University, 930 Sakaedani, Wakayama 640-8510, Japan

nakanisi@sys.wakayama-u.ac.jp

Received August 9, 2008

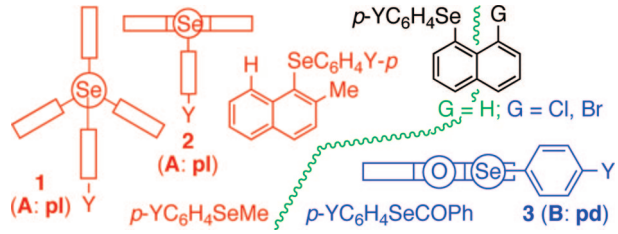

A set of new δ(Se) parameters is proposed as a standard for the planar (**pl**) orientational effect of p-YC_6H_4 (Ar) in ArSeR, employing 9-(arylselanyl)triptycenes (**1**: p-YC_6H_4SeTpc). The Se−C_R bond in ArSeR is placed on the Ar plane in **pl** and it is perpendicular to the plane in **pd**. Large upfield shifts are observed for Y = NMe_2, OMe, and Me (−22 to −6 ppm) and large downfield shifts for Y = COOEt, CN, and NO_2 (19−37 ppm), relative to Y = H, with small upfield and moderate downfield shifts by Y of halogens (−1 ppm for Y = F and 4 ppm for Y = Cl and Br). This must be the result of the p(Se)−$\pi(C_6H_4)$−p(Y) conjugation in **1** (**pl**). While the character of δ(Se) in **1** (**pl**) is very similar to that in 9-(arylselanyl)anthracenes (**2** (**pl**)), it is very different from that of 1-(arylselanyl)anthraquinones (**3** (**pd**)). Sets of δ(Se) of **1** and **2** must serve as the standard for **pl** and that of **3** does for **pd** in solutions. Structures of various ArSeR in solutions are determined from the viewpoint of the orientational effect based on the standard δ(Se) of **1**−**3**. While the structure of 2-methyl-1-(arylselanyl)naphthalenes is concluded to be all **pl** in solutions, those of 8-chloro- and 8-bromo-1-(arylselanyl)naphthalenes are all **pd**, except for Y = COOEt, CN, and NO_2: The equilibrium between **pd** and **pl** contributes to those with Y = COOEt, CN, and NO_2. The structure of 1-(arylselanyl)naphthalenes changes depending on Y. The structures of ArSeMe and ArSeCOPh are shown to be **pl** and **pd**, respectively, in solutions. Those of ArSePh and ArSeAr seem to change depending on Y. δ(Se) of **1**−**3** are demonstrated to serve as the standard to determine the structures in solutions. The rules of thumb derived from the characters in δ(Se) for **1**−**3** are very useful to determine the structures of ArSeR in solutions, in addition to the analysis based on the plots.

Introduction

NMR spectroscopy has been established as an extremely powerful tool to study physical, chemical, and biological sciences.[1,2] NMR chemical shifts (δ) are widely applied to determine structures[2−5] and follow reactions routinely.[1,2] ^{77}Se NMR chemical shifts (δ(Se)) are widely applied to determine the structures, since they are very sensitive to structural changes of selenium compounds.[2−5] We often worry about the structures of compounds in solutions, when investigations are carried out in solutions, even if the structures are determined in crystals. Plain rules are necessary to determine geometric and electronic structures based on δ(Se) in solutions, which must be founded on theoretical background and familiar to experimental chemists.

* To whom correspondence should be addressed. Phone: +81 73 457 8252. Fax: +81 73 457 8253.

(1) (a) *Organic Selenium Compounds: Their Chemistry and Biology*; Klayman, D. L., Günther, W., Eds.; Wiley: New York, 1973. (b) *The Chemistry of Organic Selenium and Tellurium Compounds*; Patai, S., Rappoport, Z., Eds.; John-Wiley and Sons: New York, 1986; Vols. 1 and 2. (c) *Organic Selenium Chemistry*; Liotta, D., Ed.; Wiley-Interscience: New York, 1987. (d) *Organoselenium Chemistry, A practical Approach*; Back, T. G., Ed.; Oxford University Press: Oxford, UK, 1999. (e) *Organoselenium Chemistry Modern Developments in Organic Synthesis*; Topics in Current Chemistry Series; Wirth, T., Ed.; Springer: New York, 2000.

10.1021/jo801786j CCC: $40.75 © 2008 American Chemical Society
Published on Web 11/06/2008

SCHEME 1. The pd, pl, and np Notation in the Benzene System and Types A−C in the Naphthalene System

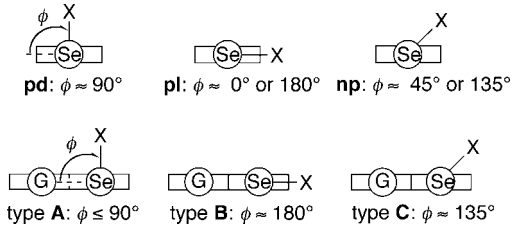

Charge-transfer mechanism has been proposed to explain the downfield shifts by the neighboring oxygen[6] and the mechanism is demonstrated to play an important role in weak interactions.[4] Other mechanisms must also be important when the structures are discussed based on the observed δ(Se) values. We pointed out the importance of the orientational effect, for better understanding the structures of *p*-YC_6H_4SeR (ArSeR) in solutions based on δ(Se).[5]

Odom tried to explain δ(Se) of *p*-$YC_6H_4SeCOPh$ based on those of related compounds such as *p*-YC_6H_4SeMe.[3b] However, the effort was not successful. We wondered if the orientational effect must be responsible for the results: The electronic effect on δ(Se) of *p*-$YC_6H_4SeCOPh$ must be very different from that on δ(Se) of *p*-YC_6H_4SeMe due to the different orientational effects for the two. Such effect was seldom discussed in the substituent effect.[7]

Typical conformers in relation to the orientational effect of ArSeR are planar (**pl**) and perpendicular (**pd**) conformers, where the Se−C_R bond in ArSeR is on the Ar plane in **pl** and it is perpendicular to the plane in **pd**.[8,9] Scheme 1 shows **pl** and **pd** notation, together with **np** (nonplanar and nonperpendicular conformer), employing ArSeX. Scheme 1 also shows the type **A** (**A**), **B**, and **C** notation[3e,4,5] exemplified by the naphthalene system, 8-G-1-(XSe)$C_{10}H_6$: The Se−X bond is placed almost perpendicular to the naphthyl plane in **A**, the bond is located on the plane in **B**, and the **C** structure is the intermediate between **A** and **B**.

CHART 1

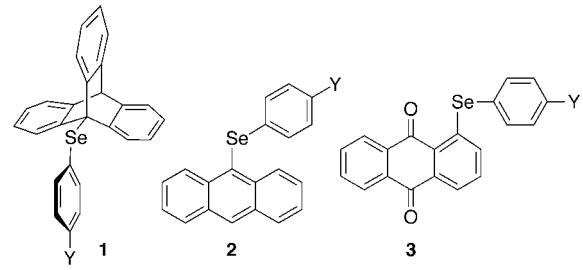

	a	b	c	d	e	f	g	h	i	j
Y =	H	NMe_2	OMe	Me	F	Cl	Br	COOEt	CN	NO_2

SCHEME 2. 1 (A: pl), 2 (A: pl), and 3 (B: pd), Together with Plausible Structures of 4−19

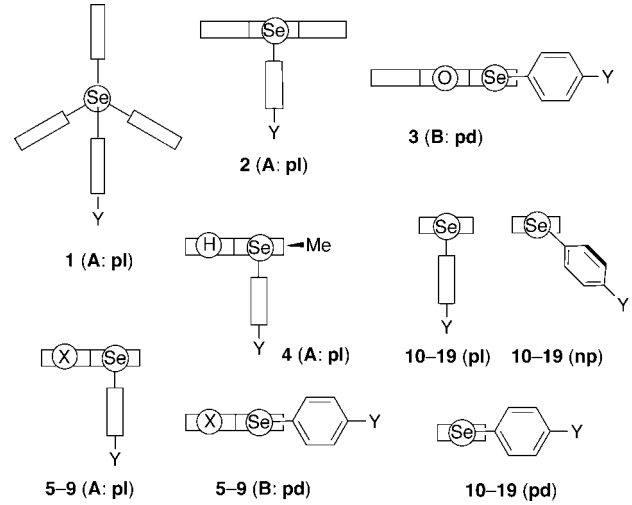

To clarify the relationship between the structures and δ(Se), it is necessary to fix the conformers of all aryl groups in ArSeR examined.[7] 9-(Arylselanyl)triptycenes (**1**: *p*-YC_6H_4SeTpc) must be an excellent candidate for **pl** where Y = H (**a**), NMe_2 (**b**), OMe (**c**), Me (**d**), F (**e**), Cl (**f**), Br (**g**), COOEt (**h**), CN (**i**), and NO_2 (**j**) at the ground state (Chart 1). Recently, we proposed sets of δ(Se) for **pl** and **pd** employing 9-(arylselanyl)anthracenes (**2**: *p*-YC_6H_4SeAtc) and 1-(arylselanyl)anthraquinones (**3**: *p*-YC_6H_4SeAtq), respectively, where Y = H (**a**), NMe_2 (**b**), OMe (**c**), Me (**d**), F (**e**), Cl (**f**), Br (**g**), COOEt (**h**), CN (**i**), and NO_2 (**j**) (Chart 1).[10] The orientational effect on δ(Se) should be firmly established for **1** in addition to **2** and **3**.

The **A**, **B**, and **C** notation is applied to the conformers of the 9-anthryl and 1-anthraquinonyl groups in **2** and **3**, respectively.[3e,4,5,8−10] The structure of **2** is **A** for the 9-anthryl group and **pl** for the substituted phenyl group, which is denoted by **2** (**A**: **pl**). That of **3** is **B** for the 1-anthraquinonyl group and **pd** for the substituted phenyl group (**3** (**B**: **pd**)). We call the ground state of **1** (**A**: **pl**) (**1** (**A**: **pl**)), after the notation of **2** (**A**: **pl**) and **3** (**B**: **pd**): The Se−C_{Ar} bond in **1** (**A**: **pl**) is on the bisected plane of two phenyl groups in the triptycyl group (see Chart 1). The set of δ(Se) of **1** (δ(Se: **1**)) must be typical for **pl**. Scheme 2 shows some plausible structures of the triptycene, anthracene, anthraquinone, naphthalene, and benzene systems, which will be discussed in this work (see also Chart 2).

The mechanisms of the orientational effect in **2** and **3** are elucidated thoroughly by employing the calculated absolute

(2) (a) MacFarlane, W.; Wood, R. J. *J. Chem. Soc., Dalton Trans.* **1972**, *13*, 1397–1401. (b) Iwamura, H.; Nakanishi, W. *J. Synth. Org. Chem. Jpn.* **1981**, *39*, 795–804. (c) *The Chemistry of Organic Selenium and Tellurium Compounds*; Patai, S., Rappoport, Z., Eds.; John-Wiley and Sons: New York, 1986; Vol. 1, Chapter. 6. (d) *Compilation of Reported ^{77}Se NMR Chemical Shifts*; Klapotke, T. M., Broschag, M., Eds.; Wiley: New York, 1996. (e) Duddeck, H. *Prog. Nucl. Magn. Reson. Spectrosc.* **1995**, *27*, 1−323.

(3) (a) Gronowitz, S.; Konar, A.; Hörnfeldt, A.-B. *Org. Magn. Reson.* **1977**, *9*, 213–217. (b) Mullen, G. P.; Luthra, N. P.; Dunlap, R. B.; Odom, J. D. *J. Org. Chem.* **1985**, *50*, 811–816. (c) Kalabin, G. A.; Kushnarev, D. F.; Bzesovsky, V. M.; Tschmutova, G. A. *J. Org. Magn. Reson.* **1979**, *12*, 598–604. (d) Kalabin, G. A.; Kushnarev, D. F.; Mannafov, T. G. *Zh. Org. Khim.* **1980**, *16*, 505–512. (e) Nakanishi, W.; Hayashi, S.; Uehara, T. *Eur. J. Org. Chem.* **2001**, *2001*, 3933–3943.

(4) (a) Hayashi, S.; Nakanishi, W. *J. Org. Chem.* **1999**, *64*, 6688–6696. (b) Nakanishi, W.; Hayashi, S.; Yamaguchi, H. *Chem. Lett.* **1996**, *94* (5), 7–948. (c) Nakanishi, W.; Hayashi, S.; Sakaue, A.; Ono, G.; Kawada, Y. *J. Am. Chem. Soc.* **1998**, *120*, 3635–3640. (d) Nakanishi, W.; Hayashi, S. *J. Org. Chem.* **2002**, *67*, 38–48.

(5) (a) Nakanishi, W.; Hayashi, S. *Chem. Lett.* **1998**, 523–524. (b) Nakanishi, W.; Hayashi, S. *J. Phys. Chem. A* **1999**, *103*, 6074–6081.

(6) Barton, D. H. R.; Hall, M. B.; Lin, Z.; Parekh, S. I.; Reibenspies, J. *J. Am. Chem. Soc.* **1993**, *115*, 5056–5059.

(7) The importance of relative conformations between substituents and probe sites in the substituent effects is pointed out. See for example: Bordwen, K.; Grubbs, E. J. Angular Dependence of Dipolar Substituent Effects. In *Progress in Physical Organic Chemistry*; Taft, R. W., Ed.; John Wiley & Sons: New York, 1993; Vol. 19, pp 183−224. See also references cited therein.

(8) Nakanishi, W.; Hayashi, S.; Uehara, T. *J. Phys. Chem. A* **1999**, *103*, 9906–9912.

(9) Hayashi, S.; Wada, H.; Ueno, T.; Nakanishi, W. *J. Org. Chem.* **2006**, *71*, 5574–5585.

(10) Nakanishi, W.; Hayashi, S.; Shimizu, D.; Hada, M. *Chem. Eur. J.* **2006**, *12*, 3829–3846.

SCHEME 3. Interconversion between Conformers in 1

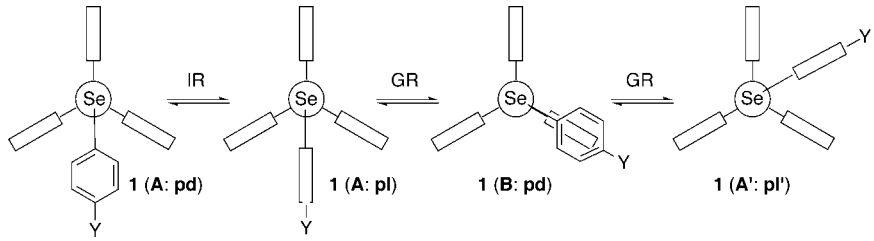

CHART 2

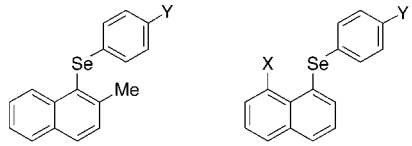

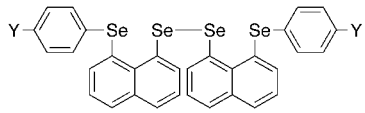

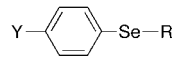

10 (R = H), **11** (R = Me), **12** (R = Ph), **13** (R = C_6H_4Y-*p*)
14 (R = CN), **15** (R = Bz), **16** (R = Br), **17** (R = $CH{=}CH_2$)
18 (R = CH=CHCl-*trans*), **19** (R = $CHCH_2CCl_2$-*cyclo*)

	a	b	c	d	e	f	g	h	i	j
Y =	H	NMe_2	OMe	Me	F	Cl	Br	COOEt	CN	NO_2

paramagnetic shielding tensors (σ^p(Se)).[11] The proposed δ(Se: **2**) and δ(Se: **3**) values should act as the standards for the orientational effect to determine the structures of ArSeR in solutions. However, the temperature dependence in δ(Se: **2**) is larger than that in δ(Se: **3**), which shows that the structure of **2** (**A**: **pl**) is less rigid relative to that of **3** (**B**: **pd**). It is worthwhile to examine the new set of δ(Se) in **1** (**A**: **pl**) before applying δ(Se: **2**) and δ(Se: **3**) to determine the structures of various ArSeR in solutions, if the temperature dependence in δ(Se: **1**) is substantially smaller than that in δ(Se: **2**). The *p*-YC_6H_4Se group in **1** is attached directly to the sp^3 carbon whereas that in **2** to the sp^2 carbon: The effect of R in *p*-YC_6H_4SeR on δ(Se) is also of interest, which is another reason to examine δ(Se: **1**) of (**A**: **pl**).

Here we propose a new set of δ(Se) for **pl** employing **1**. After confirmation of the availability of δ(Se: **1**) as the standard for **pl**, the structures in solutions are analyzed for various ArSeR (**4**−**19**) shown in Chart 2, in view of the orientational effect.[8,12]

Results and Discussion

Survey of Structure and Stereochemistry of 1. Scheme 3 shows the (**A**: **pl**), (**A**: **pd**), and (**B**: **pd**) structures and some stereochemistry in **1**. The process from **1** (**A**: **pl**) to **1** (**B**: **pd**) is called the gear rotation (GR) whereas that from **1** (**A**: **pl**) to **1** (**A**: **pd**) corresponds to the isolated rotation (IR). While the IR process changes the sites in the *p*-YC_6H_4 group, GR changes those in both *p*-YC_6H_4 and triptycyl groups. The (**A**: **pl**) structure is confirmed for **1a**, **1b**, **1c, 1f**, and **1j** by the X-ray analysis, although not shown.[13] The IR process is detected to be energetically more favored than the GR process by the dynamic ^{1}H NMR measurements for **1**,[13] together with the quantum chemical (QC) calculations.

TABLE 1. Results of QC Calculations on 1a

level	E(**A**: **pl**) (au)	ΔE(**A**: **pl**)[a] (kJ mol^{-1})	ΔE(**A**: **pd**)[a] (kJ mol^{-1})	ΔE(**B**: **pd**)[a] (kJ mol^{-1})
B3LYP[b]	−3403.3506	as 0.0	17.9	24.2
MP2[c]	−3396.0128	as 0.0	19.4	30.3

[a] Relative to (**A**: **pl**). [b] The 6-311+G(d) basis sets being employed for Se and the 6-311G(d) basis sets for C and H. [c] The 6-311+G(d) basis sets being employed for Se and the 4-31G(d) basis sets for C and H.

QC calculations are performed on **1a** (Y = H), using the Gaussian 03 program[14] at DFT (B3LYP)[15,16] and MP2[17] levels. Table 1 shows the results of QC calculations. **1a** (**A**: **pl**) is optimized as the global minimum and **1a** (**A**: **pd**) and **1a** (**B**: **pd**) are predicted to be the transition states at both B3LYP and MP2 levels. The expectations are supported by the calculations. Consequently, δ(Se: **1**) should serve as the standard for (**A**: **pl**) in the ground state. **1a** (**A**: **pd**) is predicted to be more stable than **1a** (**B**: **pd**). δ(Se) of **1** (**A**: **pl**) are determined and the efficiency as the standard for **pl** is examined next.

^{77}Se NMR Chemical Shifts and Behavior of 1. The δ(Se: **1**) values were measured in chloroform-*d* solutions (0.040 M) at the temperatures of 213, 297, and 333 K, similarly to the case of **2** and **3** (0.050 M). Table 2 shows δ(Se) for **1a**−**3a** from MeSeMe and $\delta(Se)_{SCS}$ for **1**−**3** from **1a**−**3a**, the parent selenium compounds with Y = H, respectively. Characteristic points of **1** (**A**: **pl**) are summarized as follows: Large upfield shifts are observed for Y = NMe_2, OMe, and Me (−22 to −6 ppm) and large downfield shifts for Y = COOEt, CN, and NO_2 (19−37 ppm) relative to Y = H, with small upfield and moderate downfield shifts by Y of halogens (−1 ppm for Y =

(11) (a) *Encyclopedia of Nuclear Magnetic Resonance*; Grant, D. M., Harris, R. K., Eds.; John Wiley & Sons: New York, 1996. (b) *Nuclear Magnetic Shieldings and Molecular Structure*; Tossell, J. A., Ed.; Kluwer Academic Publishers: Dordrecht, The Netherlands, 1993. (c) Calculation of NMR and EPR Parameters. *Theory and Applications*; Kaupp, M., Bühl, M., Malkin, V. G., Eds.; Wiley-VCH Verlag GmbH & Co. KGaA: Weinheim, Germany, 2004. (d) *Spins in Chemistry*; McWeeny, R., Ed.; Academic Press: New York, 1970. (e) Markin, V. G.; Malkina, O. L.; Eriksson, L. A. A Tool for Chemistry. In *Modern Density Functional Theory*; Seminario, J. M., Politzer, P., Eds.; Elsever: Amsterdam, The Netherlands, 1994. (f) *Density-functional Methods in Chemistry and Material Science*; Springborg, M., Ed.; John Wiley & Sons: New York, 1977.

(12) Hayashi, S.; Yamane, K.; Nakanishi, W. *J. Org. Chem.* **2007**, *72*, 7587–7596.

(13) The dynamic ^{1}H NMR spectroscopy was applied on **1**. The ground state nature of **1** (**A**: **pl**) is established. These results are in accordance with those obtained based on δ(Se). Details of the dynamic stereochemistry based on the temperature-dependent ^{1}H NMR spectroscopy for **1**, together with the structures, will be reported elsewhere.

(14) Frisch, M. J. et al. *Gaussian 03*, revision D.02; Gaussian, Inc.: Wallingford, CT, 2004.

(15) (a) Lee, C.; Yang, W.; Parr, R. G. *Phys. Rev. B* **1988**, *37*, 785–789. (b) Miehlich, B.; Savin, A.; Stoll, H.; Preuss, H. *Chem. Phys. Lett.* **1989**, *157*, 200–206.

(16) (a) Becke, A. D. *Phys. Rev. A* **1988**, *38*, 3098–3100. (b) Becke, A. D. *J. Chem. Phys.* **1993**, *98*, 5648–5652.

(17) (a) Møller, C.; Plesset, M. S. *Phys. Rev.* **1934**, *46*, 618–622. (b) Gauss, J. *J. Chem. Phys.* **1993**, *99*, 3629–3643. (c) Gauss, J. *Ber. Bunsenges., Phys. Chem.* **1995**, *99*, 1001–1008.

TABLE 2. Observed $\delta(Se)_{SCS}$ of 1−3[a]

compd	T (K)	NMe_2 (**b**)	OMe (**c**)	Me (**d**)	H (**a**)	F (**e**)	Cl (**f**)	Br (**g**)	CO_2Et (**h**)	CN (**i**)	NO_2 (**j**)
1	213	−21.63	−11.61	−5.93	0.00 (257.13)	−0.71	3.74	4.16	18.69	29.90	36.56
1	297	−20.45	−11.24	−5.95	0.00 (258.97)	−0.66	3.68	4.14	17.20	28.62	33.67
1	333	−20.03	−11.06	−5.98	0.00 (259.63)	−0.76	3.55	3.97	16.47	27.93	32.41
2[b]	213	−22.7	−12.7	−6.3	0.0 (245.3)	−3.3	1.9	2.4	17.4	27.7	32.7
2[b]	297	−21.0	−12.2	−6.6	0.0 (249.0)	−3.6	1.5	1.6	16.2	26.2	30.4
2[b]	333	−21.3	−12.7	−6.8	0.0 (250.6)	−3.9	1.0	1.2	15.2	24.8	29.0
3[b]	213	−20.6	−15.5	−9.2	0.0 (511.4)	−10.5	−7.1	−6.4	0.1	8.5	2.7
3[b]	297	−19.6	−15.0	−9.0	0.0 (512.3)	−10.2	−7.1	−6.4	0.0	8.2	2.5
3[b]	333	−19.5	−15.0	−9.1	0.0 (512.5)	−10.3	−7.2	−6.7	−0.3	7.9	2. 2

[a] $\delta(Se)_{SCS}$ are given for **1**−**3** and δ(Se) for **1a**−**3a** in parentheses, measured in chloroform-*d* (0.040 M for **1** and 0.050 M for **2** and **3**). [b] Reference 10.

F and 4 ppm for Y = Cl and Br). This must be the result of the typical p−π conjugation of the p(Se)−$\pi(C_6H_4)$−p(Y) type in **1** (**A**: **pl**). The characters of **1** (**A**: **pl**) are very similar to those of **2** (**A**: **pl**) whereas they are very different from those of **3** (**B**: **pd**). However, there are some differences between δ(Se) in **1** (**A**: **pl**) and those in **2** (**A**: **pl**): Y of halogens in **2** (**A**: **pl**) cause moderate upfield shifts by Y = F (−4 ppm) and small downfield shifts by Y = Cl and Br (1−2 ppm). The differences would be ascribed to the sp^3 versus sp^2 carbon atoms attached directly to the *p*-YC_6H_4Se groups in **1** and **2**, respectively.

The higher temperature dependence of δ(Se) in **2** (**A**: **pl**) relative to **3** (**B**: **pd**) has been pointed out.[10] The results strongly suggest that the global minima of **3** (**B**: **pd**) are thermally very stable and the (**B**: **pd**) structure is exclusive for all Y examined in **3**; however, **2** (**A**: **pl**) would fluctuate around the global minima. **2** (**A**: **pl**) could equilibrate slightly with **2** (**B**: **pd**) for Y of strong donors such as NMe_2. The p−π conjugation of the p(Se)−$\pi(C_6H_4)$−p(Y) type affects the stability of the conformers. Therefore, Y of acceptors stabilize (**A**: **pd**) through the favorable p−π conjugation, whereas Y of donors will destabilize (**A**: **pd**) through unfavorable interactions between electron-rich p(Se) and p(Y), which would facilitate the equilibrium between (**A**: **pd**) and (**B**: **pd**). The δ(Se) values and the temperature dependence must be carefully examined especially for Y of strong donors such as Y = NMe_2 and/or OMe.

What are the δ(Se) values and the temperature dependence in **1** (**A**: **pl**)? δ(Se) of **1a** (Y = H) at 213 K is 257.13 relative to MeSeMe: The value shifts downfield by 2.50 ppm when the temperature goes up to 333 K under the measurement conditions (relative to MeSeMe).[18] The value of 2.50 ppm for **1a** is 0.47 times larger than that in **2a** (5.3 ppm)[19] for the temperature range of 213−333 K. The smaller temperature dependence of δ(Se: **1a**) relative to δ(Se: **2a**) must show that the **1** (**A**: **pl**) structure is more rigid than the case of **2**, under the measurement conditions containing the temperature change. δ(Se) of **1b** (Y = NMe_2) are 235.50 (257.13 − 21.63) and 239.60 at 213 and 333 K, respectively, and those of **1j** (Y = NO_2) are 293.69 and 292.04, respectively. Consequently, δ(Se) of **1b** (Y = NMe_2) and **1j** (Y = NO_2) move downfield and upfield by 4.10 and 1.65 ppm, respectively, when the temperature goes up from 213 to 333 K. Similarly, δ(Se) of **2b** (Y = NMe_2) and **2j** (Y = NO_2) move downfield and upfield by 6.7 (229.3 − 222.6) and 1.6 ppm,[19] respectively, when the temperature goes up from 213 to 333 K. The temperature dependence in δ(Se: **1b**) (4.10 ppm) is substantially smaller than that of δ(Se: **2b**) (6.7 ppm), which shows that the (**A**: **pl**) structure is more stable in **1** than the case of **2**, under the measurement conditions.

$\delta(Se)_{SCS}$ for **1b** (Y = NMe_2) and **1j** (Y = NO_2) shift downfield and upfield by 1.60 and 4.15 ppm, respectively, when the temperature changes from213 to 333 K (relative to **1a**). Similarly, $\delta(Se)_{SCS}$ for **2b** (Y = NMe_2) and **2j** (Y = NO_2) shift downfield and upfield by 1.4 and 3.7 ppm, respectively, when the temperature changes from 213 to 333 K (relative to **2a**). The substituent effect on the temperature dependence in **1** and **2** is almost equal. Consequently, the temperature dependence can be discussed based on δ(Se: **1a**) and δ(Se: **2a**), which is discussed above. These results strongly support that the (**A**: **pl**) structure in **1** is stable enough to employ δ(Se: **1**) as the standard of **pl**.[13]

TABLE 3. Correlations in $\delta(Se)_{SCS}$ of 1−3[a]

entries	correlation	a	b	r^2	n
1	δ(Se: **1**)$_{SCS:297}$ vs δ(Se: **1**)$_{SCS:213}$	0.9394	−0.09	0.9996	10
2	δ(Se: **1**)$_{SCS:333}$ vs δ(Se: **1**)$_{SCS:213}$	0.9128	−0.20	0.9992	10
3	δ(Se: **2**)$_{SCS:333}$ vs δ(Se: **2**)$_{SCS:213}$	0.9155	−0.75	0.9996	10
4	δ(Se: **3**)$_{SCS:333}$ vs δ(Se: **3**)$_{SCS:213}$	0.9463	−0.31	0.9994	10
5	δ(Se: **2**)$_{SCS:213}$ vs δ(Se: **1**)$_{SCS:213}$	0.960	−1.4	0.998	10
6	δ(Se: **3**)$_{SCS:213}$ vs δ(Se: **1**)$_{SCS:213}$	0.541	−8.7	0.989	8[b]

[a] The constants (a, b, r^2) are defined by eq 1 in the text. [b] Neglecting the data for Y = H and NO_2.

To examine the temperature dependence of **1** further, δ(Se: **1**) at 297 and 333 K are plotted versus those at 213 K. Plots are analyzed according to eq 1. Table 3 collects the a, b, and r^2 values for the correlations (entries 1 and 2). The correlations are excellent (r^2 > 0.999). The results suggest that the temperature dependence of δ(Se: **1**) is governed by a simple mechanism. As mentioned above, the temperature dependence of δ(Se) in **1** (**A**: **pl**) was smaller than that in **2** (**A**: **pl**) (about 0.47 times), which must be the reflection of the more stable global minima of **1** (**A**: **pl**), relative to **2** (**A**: **pl**).

$$y = ax + b \quad (r^2\text{: square of the correlation coefficient}) \quad (1)$$

We supposed that the temperature dependence of **1** would be the reflection of the extended population to larger torsional

(18) The temperature dependence of δ(Se) of MeSeMe is reported to be ca. 2.5 ppm over the temperature range of 222−323 K with a 60% chloroform solution. See: Luthra, N. P.; Dunlap, R. B.; Odom, J. D. *J. Magn. Reson.* **1983**, *52*, 318–322. In our case, δ(Se) of MeSeMe shifts downfield by 5.6 ppm for a 10% chloroform solution, relative to the frequency of the spectrometer, when the temperature changes from 213 to 333 K. The results show that the temperature dependence of **1a** is about 1.5 times of that of MeSeMe. The temperature dependence of δ(Se) of **1j** is comparable to that of MeSeMe.

(19) (Se) of **2b** (Y = NMe_2) and **2j** (Y = NO_2) move downfield by 6.7 and 1.6 ppm, respectively, relative to MeSeMe, when the temperature changes from 213 to 333 K.

TABLE 4. Observed $\delta(Se)_{SCS}$ of 4−9[a]

compd	NMe_2 (**b**)	OMe (**c**)	Me (**d**)	H (**a**)	F (**e**)	Cl (**f**)	Br (**g**)	CO_2Et (**h**)	CN (**i**)	NO_2 (**j**)
4[b]		−11.5	−6.2	0.0 (274.6)		1.1	1.4	15.0		29.2
5[c]	−17.2	−6.8	−4.8	0.0 (361.0)	−5.0	−1.6	−1.7	7.0	13.8	18.6
6[d]		−14.9	−9.1	0.0 (460.1)		−6.3	−5.7	3.9		15.4
7[d]		−14.0	−8.6	0.0 (451.0)		−6.4	−5.9	2.7	13.2	13.4
8[e]		−9.8	−6.6	0.0 (434.3)		−2.7	−1.9	8.1		19.6
		−2.3	−0.9	0.0 (235.4)		−0.7	−0.2	3.8		4.7
9[e]		−12.8	−7.0	0.0 (429.0)		0.1	0.6	13.5		27.1

[a] $\delta(Se)_{SCS}$ are given for **4**−**9**, together with δ(Se) for **4a**−**9a** in parentheses, measured in chloroform-*d*. [b] Reference 12. [c] References 10 and 12. [d] Reference 4d. [e] Reference 4a.

angles around the energy minima due to the relatively shallow energy surface. The temperature dependence in solvation must also affect the dependence of δ(Se).

Basic behaviors of δ(Se) for **2** (**A**: **pl**) and **3** (**B**: **pd**) are discussed in the preceding paper.[10] The plots of δ(Se: **2**)$_{SCS:333}$ versus δ(Se: **2**)$_{SCS:213}$ and δ(Se: **3**)$_{SCS:333}$ versus δ(Se: **3**)$_{SCS:213}$ gave excellent correlations, which are also shown in Table 3 for convenience of comparison (entries 3 and 4, respectively: $r^2 > 0.999$). $\delta(Se)_{SCS}$ of **2** (**A**: **pl**) and **3** (**B**: **pd**) are plotted versus those of **1** (**A**: **pl**). Panels a and b of Figure 1 show the plots of δ(Se: **2**)$_{SCS:213}$ versus δ(Se: **1**)$_{SCS:213}$ and δ(Se: **3**)$_{SCS:213}$ versus δ(Se: **1**)$_{SCS:213}$, respectively. The former gave a very good correlation ($r^2 = 0.998$: Figure 1a): The difference between δ(Se: **1**)$_{SCS}$ and δ(Se: **2**)$_{SCS}$ for Y of halogens must be responsible for r^2 slightly smaller than 1.000. A good correlation was also obtained for the latter (Figure 1b), although data corresponding to Y = H and NO_2 deviated from the correlation. Table 3 collects the correlations (entries 5 and 6, respectively).

Compilation of these results, the rules of thumb, which are useful to examine the structures of ArSeR in solutions in view of the orientational effect based on δ(Se: **1**)$_{SCS}$, δ(Se: **2**)$_{SCS}$, and δ(Se: **1**)$_{SCS}$ as the standards, are summarized as follows: (1) For **1** (**A**: **pl**), δ(Se: **1e**: Y = F) is very close to δ(Se: **1a**: Y = H) with δ(Se: **1f**: Y = Cl) and δ(Se: **1g**: Y = Br) also close to δ(Se: **1a**). (2) δ(Se: **2f**: Y = Cl) and δ(Se: **2g**: Y = Br) are very close to δ(Se: **1a**) for **2** (**A**: **pl**). (3) In the case of **3** (**B**: **pd**), δ(Se: **3h**: Y = COOEt) is very similar to δ(Se: **3a**) and δ(Se: **3i**: Y = CN) is more downfield of δ(Se: **1j**: Y = NO_2). (4) Indeed, δ(Se) of **3** (**B**: **pd**) correlates well with δ(Se) of **1** (**A**: **pl**) (and **2** (**A**: **pl**)), except for Y = H and NO_2, but the magnitude of the *y*-intercept (*b* in eq 1) is evaluated to be large (around 9 ppm) even if data corresponding to Y = H and NO_2 are neglected. (5) The points corresponding to Y = H, Me, and OMe seem to align linearly in the plot of δ(Se: **3**) (**pd**) versus δ(Se: **1** or **2**) (**pl**) (see Figure 1b). The rules of thumb are applied to examine the structure of *p*-YC_6H_4SeR in solutions, in addition to the plot for each compound in question.

How can the structures of the naphthalene system be determined based on $\delta(Se)_{SCS}$ in solutions from the view of the orientational effect? $\delta(Se)_{SCS}$ values of **4**−**9** are analyzed based on those of **1**−**3**, first.

Structures of the Naphthalene System in Solutions Analyzed Based on $\delta(Se)_{scs}$. Table 4 collects $\delta(Se)_{SCS}$ of the naphthalene system, **4**−**9**. To organize the process for the analysis, δ(Se: **9**)$_{SCS}$ are plotted versus δ(Se: **4**)$_{SCS}$ and δ(Se: **7**)$_{SCS}$ are versus δ(Se: **6**)$_{SCS}$. The correlations are given in Table 5 (entries 1 and 2, respectively). The correlations are excellent ($r^2 \geq 0.999$). The results show that the structure of each member in **9** is very close to that of **4** and the structure of **7** to that of **6**, in solutions. Therefore, the structures of **4** (or **9**), **5**, **6** (or **7**), and **8** should be analyzed from the viewpoint of the orientational effect. δ(Se: **1**)$_{SCS:213}$, δ(Se: **2**)$_{SCS:213}$, and δ(Se: **3**)$_{SCS:213}$ are employed for the analysis. The correlations are shown in Table 5. The plots versus δ(Se: **1**)$_{SCS:213}$ and δ(Se: **3**)$_{SCS:213}$ are employed for the analysis in the text.

δ(Se: **4**)$_{SCS}$ are plotted versus δ(Se: $\mathbf{1_{pl}}$)$_{SCS:213}$ and δ(Se: $\mathbf{2_{pl}}$)$_{SCS:213}$. The correlations are excellent (entries 3 and 4, respectively, in Table 5: $r^2 = 0.997$ and 1.000, respectively).

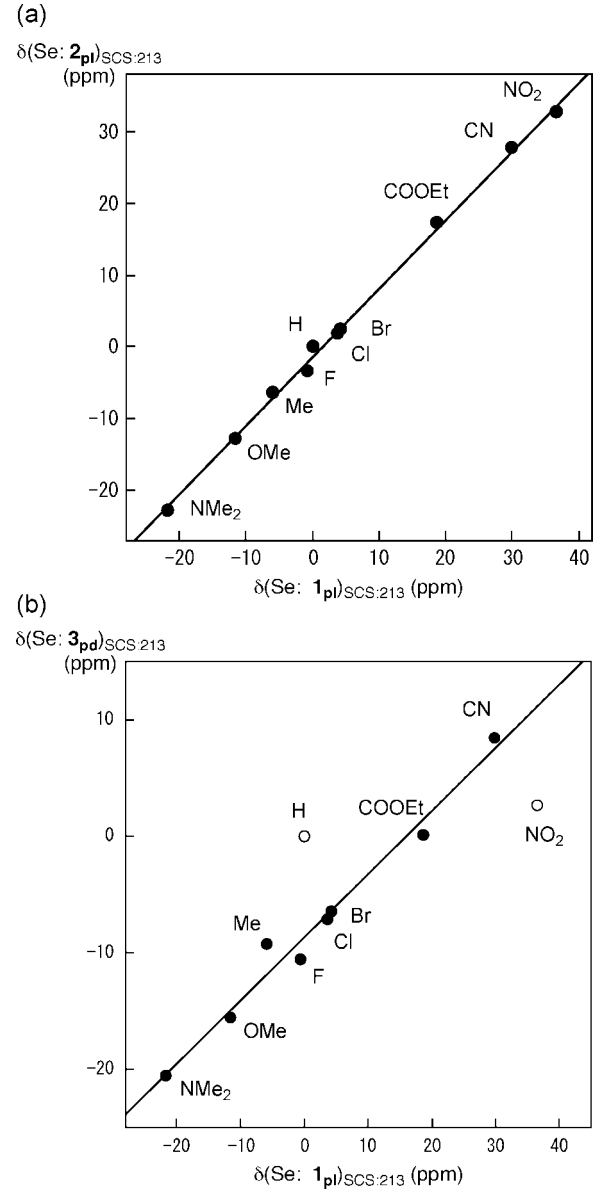

FIGURE 1. Plots of δ(Se: **2**)$_{SCS:213}$ versus δ(Se: **1**)$_{SCS:213}$ (a) and δ(Se: **3**)$_{SCS:213}$ versus δ(Se: **1**)$_{SCS:213}$ (b).

TABLE 5. Correlations between δ(Se)$_{SCS}$ in 2−9, together with 1[a]

entries	correlation	*a*	*b*	r^2	*n* (Y)
1	δ(Se: **9**)$_{SCS\text{-}Ar}$ vs δ(Se: **4**)$_{SCS}$	0.969	−0.9	0.999	7
2	δ(Se: **7**)$_{SCS}$ vs δ(Se: **6**)$_{SCS}$	0.904	−0.5	0.999	7
3	δ(Se: **4**)$_{SCS}$ vs δ(Se: **1**)$_{SCS:213}$	0.842	−1.3	0.997	7
4	δ(Se: **4**)$_{SCS}$ vs δ(Se: **2**)$_{SCS:213}$	0.898	−0.4	1.000	7
5	δ(Se: **7**)$_{SCS}$ vs δ(Se: **3**)$_{SCS:213}$	0.906	−0.1	0.999	5[b]
6	δ(Se: **5**)$_{SCS}$ vs δ(Se: **1**)$_{SCS:213}$	0.618	−4.3	0.999	6[c]
7	δ(Se: **5**)$_{SCS}$ vs δ(Se: **1**)$_{SCS:213}$	0.777	0.4	0.972	4[d]
8	δ(Se: **5**)$_{SCS}$ vs δ(Se: **2**)$_{SCS:213}$	0.634	−3.1	0.995	6[c]
9	δ(Se: **5**)$_{SCS}$ vs δ(Se: **2**)$_{SCS:213}$	0.735	0.5	0.963	4[d]
10	δ(Se: **8**)$_{SCS\text{-}Ar}$ vs δ(Se: **1**)$_{SCS:213}$	0.674	−4.9	0.999	4[e]
11	δ(Se: **8**)$_{SCS\text{-}Ar}$ vs δ(Se: **1**)$_{SCS:213}$	0.846	−0.5	0.966	3[f]
12	δ(Se: **8**)$_{SCS\text{-}Ar}$ vs δ(Se: **2**)$_{SCS:213}$	0.714	−3.9	0.999	4[e]
13	δ(Se: **8**)$_{SCS\text{-}Ar}$ vs δ(Se: **2**)$_{SCS:213}$	0.771	−0.6	0.960	3[f]
14	δ(Se: **8**)$_{SCS\text{-}Ar}$ vs δ(Se: **3**)$_{SCS:213}$	2.096	11.4	0.941	4[e]
15	δ(Se: **8**)$_{SCS\text{-}Ar}$ vs δ(Se: **3**)$_{SCS:213}$	0.638	−0.2	0.992	3[f]

[a] The constants (*a*, *b*, r^2) are defined by eq 1 in the text. [b] Y = OMe, Me, H, Cl, and Br. [c] Y = F, Cl, Br, COOEt, CN, and NO_2. [d] Y = NMe_2, OMe, Me, and H. [e] Y = Cl, Br, COOEt, and NO_2. [f] Y = OMe, Me, and H.

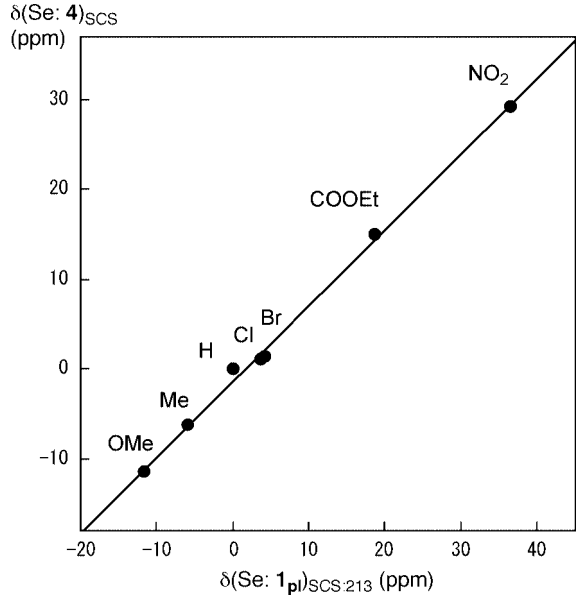

FIGURE 2. Plot of δ(Se: **4**)$_{SCS}$ versus δ(Se: **1**$_{pl}$)$_{SCS:213}$.

Figure 2 shows the plot of δ(Se: **4**)$_{SCS}$ versus δ(Se: **1**$_{pl}$)$_{SCS:213}$. The structures are concluded to be **pl** for all members in **4** and **9** in solutions.

δ(Se: **7**)$_{SCS}$ are plotted versus δ(Se: **3**$_{pd}$)$_{SCS:213}$ next. Figure 3 shows the results. An excellent correlation is obtained for Y = OMe, Me, H, Cl, and Br ($r^2 \geq 0.999$): The correlation with Y = OMe, Me, H, Cl, and Br is shown in Table 5 (entry 5). Data for Y = COOEt deviate slightly from the correlation and

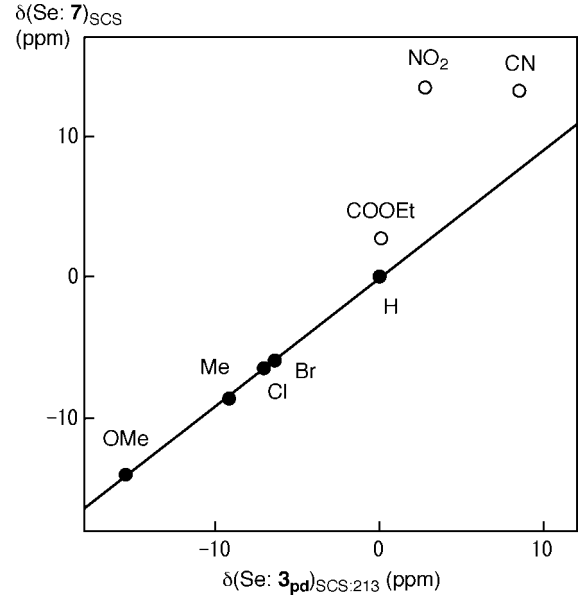

FIGURE 3. Plot of δ(Se: **7**)$_{SCS}$ versus δ(Se: **3**$_{pd}$)$_{SCS:213}$.

those for Y = CN and NO_2 do substantially. δ(Se: **7h**: Y = COOR) is fairly close to δ(Se: **7a**). The results demonstrate that the structure of **7** is all **pd**, except for Y = COOEt, CN, and NO_2; while **pd** in **7** is slightly equilibrated with **pl** for Y = COOEt, **pd** and **pl** are substantially equilibrated for Y = CN and NO_2. The conclusion obtained for **7** must also be effective for **6** in solutions.

Why do **6** and **7** equilibrate between **pd** and **pl** in solutions for Y = CN and NO_2? The driving force for the (**B**: **pd**) structures of **6** and **7** is the energy lowering effect through the hypervalent 3c−4e interaction of the n_p(X)---σ*(Se−C) type (X = Cl and Br). Similarly, that of **3** (**B**: **pd**) is the hypervalent 3c−4e interaction of the n_p(O)---σ*(Se−C) type. The p−π conjugation of the p(Se)−π(Atc)−π(C═O) type assists strongly to stabilize **3** (**B**: **pd**) in addition to the hypervalent 3c−4e interaction in **3** (**B**: **pd**). Namely, the driving force to stabilize **3** (**B**: **pd**) is very strong whereas that in **6** and **7** would not be so strong. Consequently, **6** and **7** cannot exist exclusively as (**B**: **pd**) for Y = CN and NO_2 (and Y = COOEt). They equilibrate between (**B**: **pd**) and (**A**: **pl**) in solutions. Scheme 4 explains the interactions.

δ(Se: **5**)$_{SCS}$ are plotted versus δ(Se: **1**$_{pl}$)$_{SCS:213}$, δ(Se: **2**$_{pl}$)$_{SCS:213}$, and δ(Se: **3**$_{pd}$)$_{SCS:213}$ next. Panels a and b in Figure 4 show the plots versus δ(Se: **1**$_{pl}$)$_{SCS:213}$ and δ(Se: **3**$_{pd}$)$_{SCS:213}$, respectively. The plot in Figure 4a is analyzed by two groups: Data with Y = NMe_2, OMe, Me, and H make up one group and those with Y = NO_2, CN, COOEt, Br, Cl, and F belong to another. The correlations are given in Table 5 (entries 6−9). Correlations seem poor in the plot versus δ(Se: **3**$_{pd}$)$_{SCS}$ (Figure 4b). One might conclude that the structure of **5** is (**A**, **pl**) for Y = NO_2, CN, COOEt, Br, Cl, and F in solutions at first glance. However, the correlation must be carefully examined, since the *b* values are −3.1 to −4.3, which are not close to 0.0 (see entries 6 and 8 in Table 5). The structure of **5** should be exclusively (**A**: **pl**) for Y = NO_2 and CN; however, the equilibrium between (**A**: **pl**) and (**B**: **pd**) contribute gradually in solutions as the acceptor ability of Y becomes weaker, although the plot gives an excellent correlation for Y = NO_2, CN, COOEt, Br, Cl, and F. Finally (**B**: **pd**) would be predominant for Y = NMe_2 (and Y = OMe) in solutions. The equilibrium would substantially contribute to the structure of **5** with Y = H, Me, and halogens.

SCHEME 4. Driving Force for the Formation of (B: pd) in 3, 6, and 7

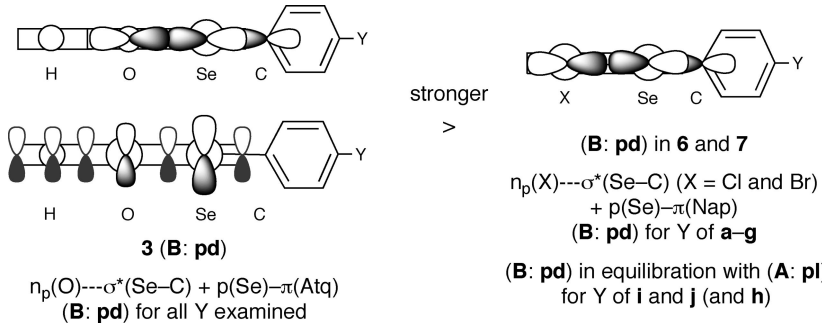

3 (**B**: **pd**)

n_p(O)---σ*(Se–C) + p(Se)–π(Atq)
(**B**: **pd**) for all Y examined

(**B**: **pd**) in **6** and **7**

n_p(X)---σ*(Se–C) (X = Cl and Br)
+ p(Se)–π(Nap)
(**B**: **pd**) for Y of **a**–**g**

(**B**: **pd**) in equilibration with (**A**: **pl**)
for Y of **i** and **j** (and **h**)

Three conformers should be in equilibrium for **8** in solutions, as shown in eq 2. Conformer **8** (**AB**-1) will be stabilized by Y of strong donors such as Y = OMe, **8** (**AB**-2) by acceptors such as Y = NO_2, and **8** (**CC**) by Y of electronically neutral groups such as H. δ(Se: **8**)$_{SCS}$ are plotted versus δ(Se: $\mathbf{1_{pl}}$)$_{SCS:213}$, δ(Se: $\mathbf{2_{pl}}$)$_{SCS:213}$, and δ(Se: $\mathbf{3_{pd}}$)$_{SCS:213}$. Panels a and b of Figure 5 show the plots of δ(Se: **8**)$_{SCS}$ versus δ(Se: $\mathbf{1_{pl}}$)$_{SCS:213}$ and δ(Se: $\mathbf{3_{pd}}$)$_{SCS:213}$, respectively. The plots are analyzed as two correlations. An excellent correlation is obtained for Y = NO_2, COOEt, Br, and Cl in the plot of δ(Se: **8**)$_{SCS}$ versus δ(Se: $\mathbf{1_{pl}}$)$_{SCS:213}$ ($r^2 \geq 0.999$), together with a good correlation for Y = OMe, Me, and H ($r^2 = 0.96-0.97$) with small b values (−0.5 to −0.6) (Figure 5a). Figure 5a is very similar to Figure 4a, although data for **8i** (Y = CN) are missing. A good correlation is obtained in the plot of δ(Se: **8**)$_{SCS}$ versus δ(Se: $\mathbf{3_{pd}}$)$_{SCS:213}$ ($r^2 \geq 0.992$) with a very small b value (−0.2) for Y = OMe, Me, and H (Figure 5b). The results strongly support that the structure of **8** is **AB**-2 for Y = NO_2, COOEt, Br, and Cl in solutions whereas it is mainly **AB**-2 for Y = OMe, Me, and H, although some equilibrium may contribute to that for **8** for Y of electronically neutral groups.

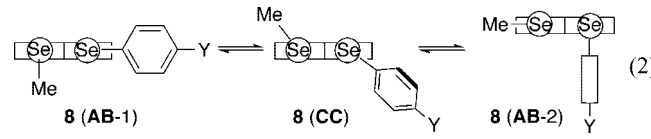

8a (Y = H), **8c** (Y = OMe), and **8f** (Y = Cl) are observed as **8** (**CC**), **8** (**AB**-1), and **8** (**AB**-2), respectively, in crystals.[8] Namely, **8** (**AB**-1) is stabilized by the n_p(Se)---σ*(Se−C) interactions for Y of donors and (**AB**-2) by those with Y of acceptors. The structure of **8** must be in equilibrium between the three conformers in solutions for Y of electronically neutral groups. The consideration is in accordance with the predicted structures in solutions.

Correlations are better with δ(Se: **2**) than δ(Se: **1**) as the standard in some cases. This is ascribed to the sp^3 versus sp^2 carbon atom attached directly to the *p*-YC_6H_4Se group in **1** versus **2**, respectively. This must be of interest as the R effect on δ(Se) of *p*-YC_6H_4SeR, although the observed differences seem small.

After clarification of the structures in solutions for the naphthalene system, the next extension is to clarify the structures of the benzene system in solutions.

Structures of the Benzene System in Solutions Analyzed Based on δ(Se)$_{scs}$. Table 6 collects the δ(Se)$_{SCS}$ values of the benzene system (**10**−**19**).[5] The δ(Se)$_{SCS}$ values of **10**−**19** are plotted versus those of **1**−**3**. Table 7 summarizes the results. The correlations versus δ(Se: **2**)$_{SCS:213}$ seem slightly better than those versus δ(Se: **1**)$_{SCS:213}$ if all data of each compound are plotted as shown in Table 7. However, the correlations versus δ(Se: **1**)$_{SCS:213}$ are better than those versus δ(Se: **2**)$_{SCS:213}$ in some cases when data of each compound are plotted separately by two groups. The plots of δ(Se: **10**−**19**)$_{SCS}$ versus δ(Se: **1**)$_{SCS:213}$ separately by the two groups, together with the correlations, are shown in Figures 6−9: The correlations versus δ(Se: **2**)$_{SCS:213}$ are given in Table S1 of the Supporting Information

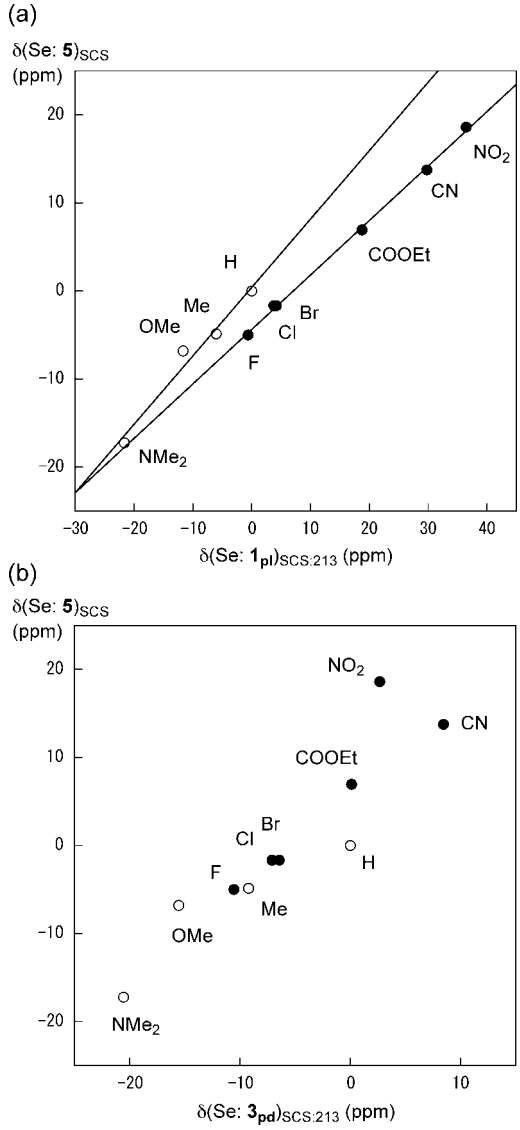

FIGURE 4. Plots of δ(Se: **5**)$_{SCS}$ versus δ(Se: $\mathbf{1_{pl}}$)$_{SCS:213}$ (a) and those versus δ(Se: $\mathbf{3_{pd}}$)$_{SCS:213}$ (b).

TABLE 6. Observed $\delta(Se)_{SCS}$ of 10−19[a,b]

compd	OMe (**c**)	Me (**d**)	H (**a**)	F (**e**)	Cl (**f**)	Br (**g**)	CO_2Et (**h**)	NO_2 (**j**)	solvent
10	−23.0	−17.0	0.0 (145)	−4.0	−3.0				neat
11	−10.4	−7.2	0.0 (207.8)		2.5	2.8	20.1[c]	33.4	$CDCl_3$
11′	−12.5	−5.9	0.0 (202.0)	−2.0	1.6		16.1[d]	31.4	neat
12	−15.5	−8.6	0.0 (423.6)		−1.7	−1.3	9.7	22.7	$CDCl_3$
13	−28.0	−16.2	0.0 (423.6)	−10.7	−3.7	−7.1	13.1	23.8	$CDCl_3$
14	−12.0	−7.8	0.0 (320.8)	−2.5	0.2	0.9	8.6	18.0	$CDCl_3$
15	−12.6	−7.1	0.0 (641.5)	−7.1	−4.5	−4.1	0.8	4.2	$CDCl_3$
16	18.7	7.9	0.0 (869.0)					−46.0	$CDCl_3$
17	−8.8	−4.6	0.0 (395.5)		−0.1	0.5		9.4	*e*
18	−6.8	−4.0	0.0 (368.6)		−2.3	−2.1		8.4	*e*
19	−13.4	−7.3	0.0 (370.2)		0.3	1.3		26.6	*e*

[a] $\delta(Se)_{SCS}$ are given for **10**−**19**, together with δ(Se) for **10a**−**19a** in parentheses. [b] Given or summarized in reference 5. [c] COOH. [d] COOME. [e] Not specified.

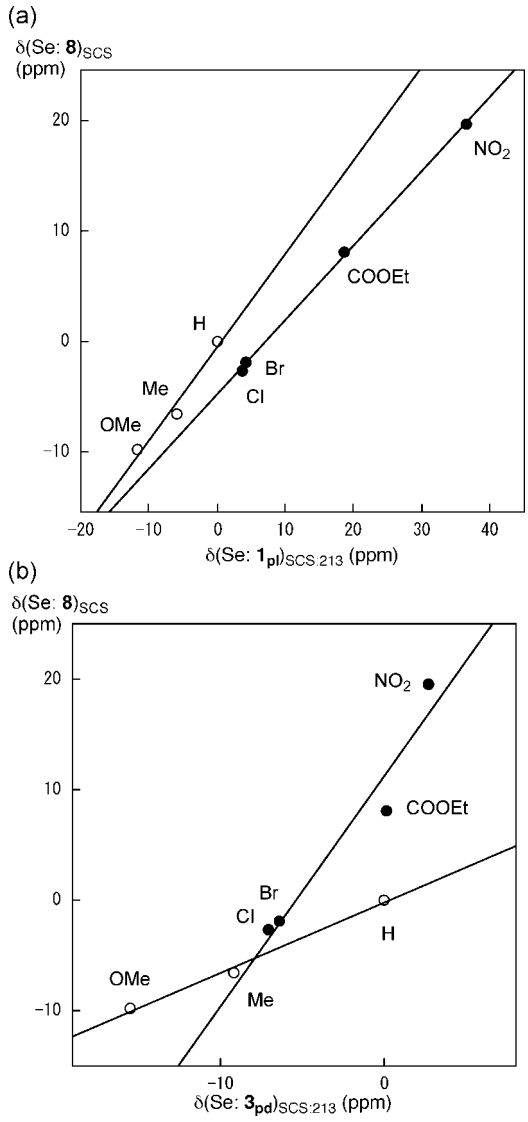

FIGURE 5. Plots of δ(Se: **8**)$_{SCS}$ versus δ(Se: $\mathbf{1_{pl}}$)$_{SCS:213}$ (a) and those versus δ(Se: $\mathbf{3_{pd}}$)$_{SCS:213}$ (b).

(SI). δ(Se: **1**)$_{SCS:213}$ and δ(Se: **3**)$_{SCS:213}$ are employed to analyze the structures of the benzene system in the text.

δ(Se: **10**)$_{SCS}$ will not be discussed, since some data needed for discussion are missing. The plots of $\delta(Se)_{SCS}$ in **11** versus δ(Se: **1**)$_{SCS:213}$ and δ(Se: **2**)$_{SCS:213}$ gave very good correlations (cf. **11′**, measured neat). The r^2 values are larger than 0.99. The plots are shown in Figure S1 in the SI. The structure of **11** should be **pl** in solutions for each member examined, although a slight equiliburium with **pd** might contribute to the structures especially for Y of strong donors.

A unique equilibrium may contribute to *p*-$YC_6H_4SeC_6H_4Y'$-*p*′ (**13′**) in solutions. Equation 3 shows the equilibrium. Conformer **13′** (C_2) is observed for Y = Y′ in crystals,[20] **13′** (**pl**) will be stabilized when the accepting ability of Y is stronger than that of Y′ and **13′** (**pd**) will be more stable than **13′** (**pl**) if Y is a stronger donor than Y′. The structures of **12** and **13** in solutions will be analyzed considering the equilibrium shown by eq 3.

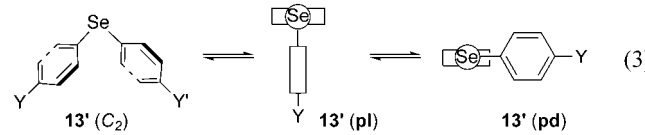

(3)

ArSePh (**12**) corresponds to **13′** with Y′ = H. Panels a and b of Figure 6 show the plot of δ(Se: **12**)$_{SCS}$ versus δ(Se: **1**)$_{SCS:213}$ and δ(Se: **3**)$_{SCS:213}$, respectively. Whereas the r^2 values are not so good if analyzed for all Y, the values become larger than 0.997 if data are analyzed separately by Y = OMe, Me, and H (Group 1) and Y = NO_2, COOEt, Br, and Cl (Group 2), except for δ(Se: **12**)$_{SCS}$ versus δ(Se: **3**)$_{SCS:213}$ for Group 2. The results show that the structure of **12** is **pl** for Group 2. However, the negative *b* value of −4.4 ppm for Group 2 in the plot of δ(Se: **12**)$_{SCS}$ versus δ(Se: **1**)$_{SCS:213}$ must be the reflection of the substantial equilibrium for Y of electronically neutral groups. The structure of **12** for Group 1 is expected to be **pd**. However, the structure is more plausible in equilibrium between **pl** and **pd** for Group 1, although **pd** would be predominant for Y = OMe.

Panels a and b of Figure 7 show the plot of δ(Se: **13**)$_{SCS}$ versus δ(Se: **1**)$_{SCS:213}$ and δ(Se: **3**)$_{SCS:213}$, respectively. Figure 7a,b is close to Figure 6a,b, respectively, although some deviations are observed in Figure 7a. δ(Se: **13**)$_{SCS}$ are all negative for Y = F, Cl, and Br and δ(Se: **13j**: Y = NO_2)$_{SCS}$ is relatively close to δ(Se: **13h**: Y = COOEt)$_{SCS}$, which must be the reflection of the substantial contribution from **pd**. This must be intrinsically observed, since if the structure of **13** is **pl** for Y it should be **pd** for Y′, where Y = Y′ in **13**. Large magnitudes of the *b* values in the plots for Group 2 support the consideration. The structure must also be in equilibrium with that of the C_2 symmetry, especially for Y of electronically neutral groups.

(20) (a) Blackmore, W. R.; Abrahams, S. C. *Acta Crystallogr.* **1955**, *8*, 323–328. (b) Klapötke, T. M.; Krumm, B.; Polborn, K. *Eur. J. Inorg. Chem.* **1999**, 1359–1366.

TABLE 7. Correlations of $\delta(Se)_{SCS}$ for 10−19 versus Those of 1−3[a]

	δ(Se: **1**)$_{SCS:213}$			δ(Se: **2**)$_{SCS:213}$			δ(Se: **3**)$_{SCS:213}$			
compd	*a*	*b*	r^2	*a*	*b*	r^2	*a*	*b*	r^2	*n*
δ(Se: **10**)$_{SCS}$	1.567	−4.9	0.871	1.625	−2.8	0.871	1.399	2.4	0.623	5
δ(Se: **11**)$_{SCS}$	0.951	−0.3	0.992	1.014	0.8	0.994	2.013	16.1	0.683	7
δ(Se: **11′**)$_{SCS}$	0.900	−1.1	0.998	0.952	0.1	0.999	1.874	14.7	0.716	7
δ(Se: **12**)$_{SCS}$	0.752	−4.1	0.973	0.804	−3.3	0.983	1.754	9.6	0.814	7
δ(Se: **13**)$_{SCS}$	1.016	−9.3	0.908	1.086	−8.0	0.929	2.468	10.6	0.886	8
δ(Se: **14**)$_{SCS}$	0.599	−2.7	0.969	0.634	−1.9	0.972	1.321	8.3	0.778	8
δ(Se: **15**)$_{SCS}$	0.305	−5.5	0.762	0.330	−5.1	0.799	0.852	1.1	0.984	8
δ(Se: **16**)$_{SCS}$	−1.309	1.4	0.997	−1.410	0.0	0.999	−2.810	−20.3	0.685	4
δ(Se: **17**)$_{SCS}$	0.346	−2.2	0.919	0.375	−1.7	0.933	0.845	4.4	0.823	6
δ(Se: **18**)$_{SCS}$	0.298	−2.5	0.936	0.324	−2.1	0.955	0.723	3.1	0.829	6
δ(Se: **19**)$_{SCS}$	0.807	−2.4	0.990	0.871	−1.4	0.996	1.783	11.8	0.727	6

[a] The constants (*a*, *b*, r^2) are defined by eq 1 in the text.

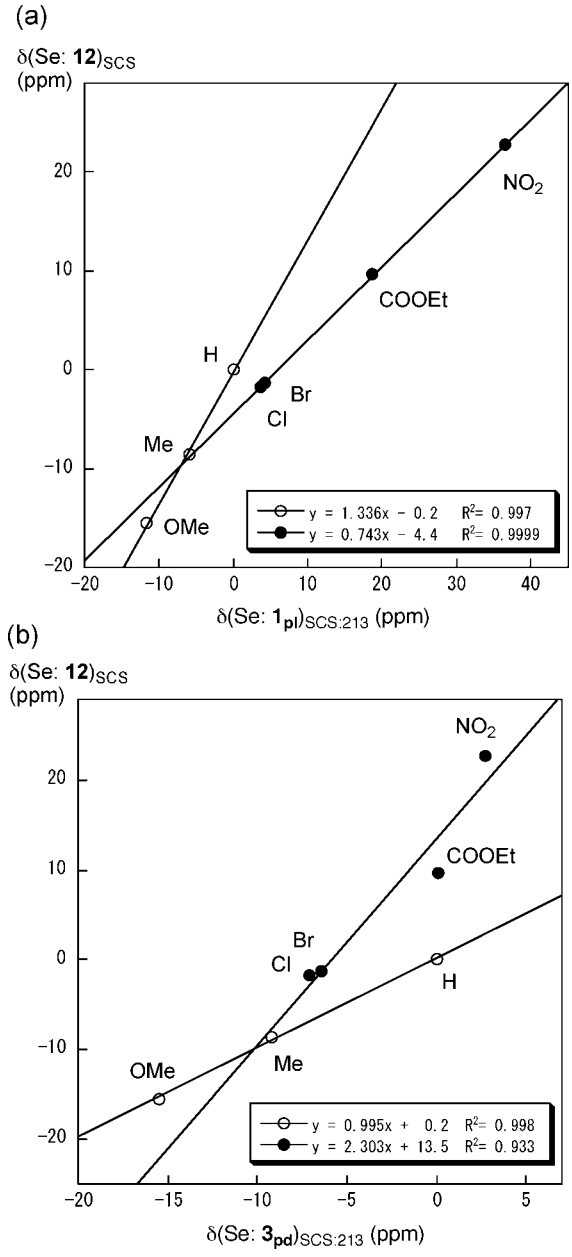

FIGURE 6. Plots of δ(Se: **12**)$_{SCS}$ versus δ(Se: **1**$_{pl}$)$_{SCS:213}$ (a) and those versus δ(Se: **3**$_{pd}$)$_{SCS:213}$ (b).

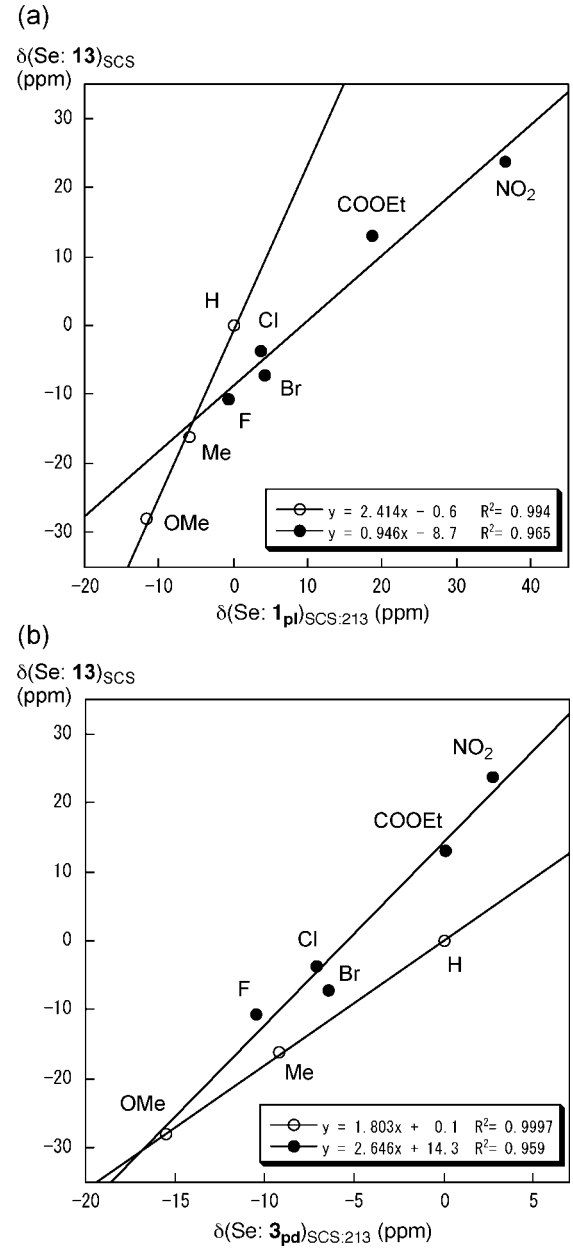

FIGURE 7. Plots of δ(Se: **13**)$_{SCS}$ versus δ(Se: **1**$_{pl}$)$_{SCS:213}$ (a) and those versus δ(Se: **3**$_{pd}$)$_{SCS:213}$ (b).

Although $\delta(Se)_{SCS}$ shift largely to upfield by Y = OMe and Me in both **pl** and **pd**, the downfield shifts by Y = COOEt and NO_2 are large only in **pl** whereas the shift values are very small in **pd** (see Table 2). The behavior seems to have an affect on the *a*

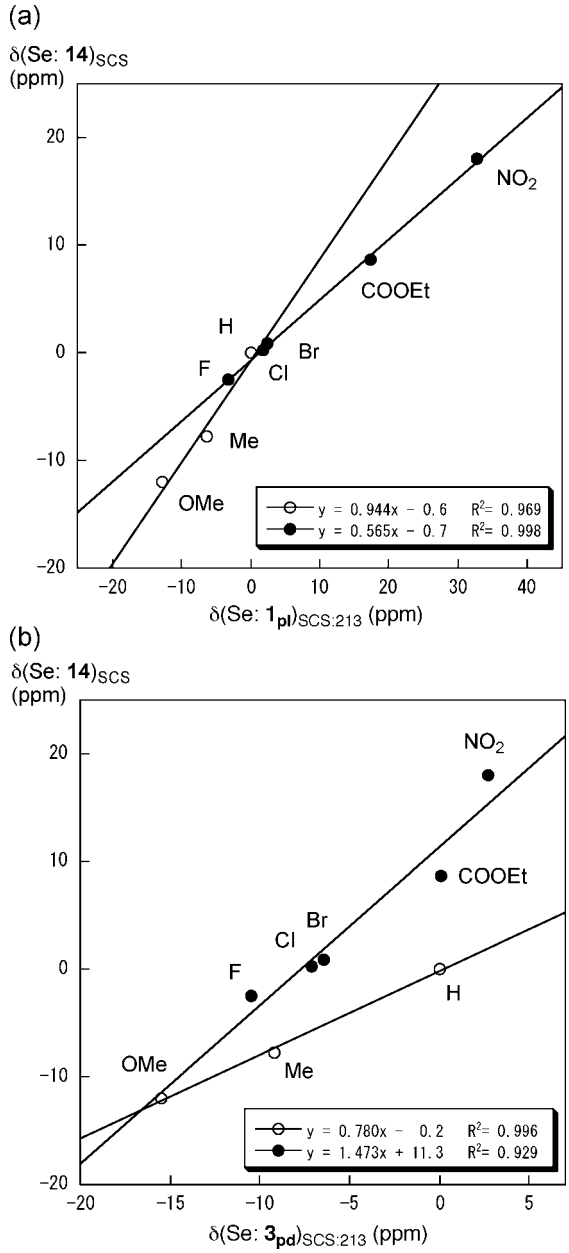

FIGURE 8. Plots of δ(Se: **14**)$_{SCS}$ versus δ(Se: $\mathbf{1_{pl}}$)$_{SCS:213}$ (a) and those versus δ(Se: $\mathbf{3_{pd}}$)$_{SCS:213}$ (b).

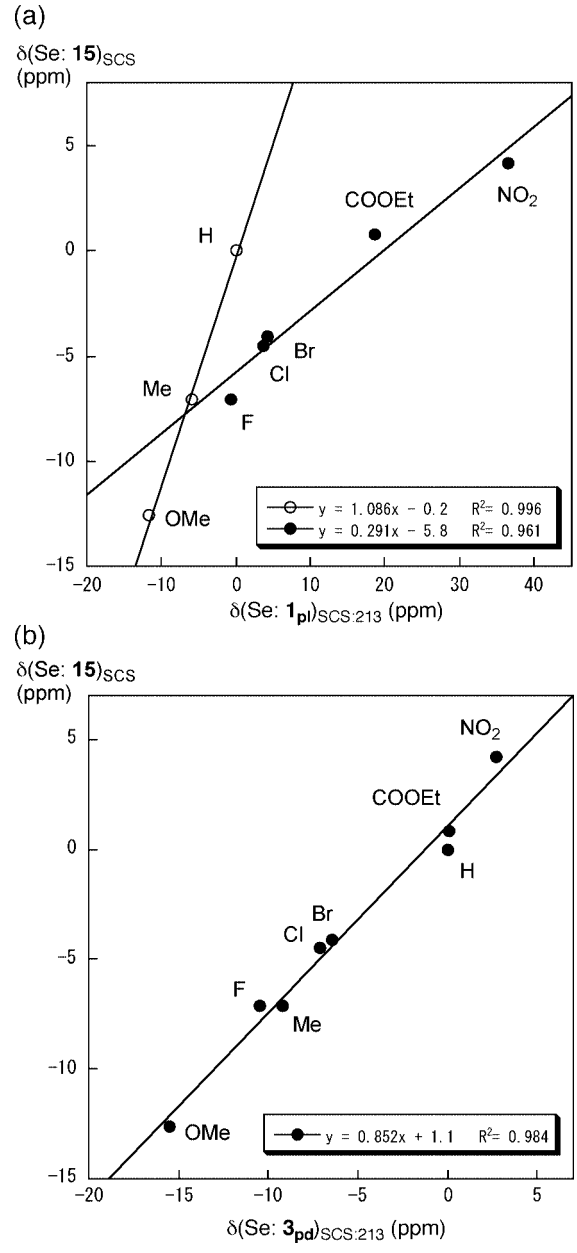

FIGURE 9. Plots of δ(Se: **15**)$_{SCS}$ versus δ(Se: $\mathbf{1_{pl}}$)$_{SCS:213}$ (a) and those versus δ(Se: $\mathbf{3_{pd}}$)$_{SCS:213}$ (b).

values in the plots of δ(Se: **11**−**13**)$_{SCS}$ versus δ(Se: **1**)$_{SCS:213}$. While the *a* values are 0.951 (**11**), 1.336 (**12**), and 2.414 (**13**) for Group 1 (Y = OMe, Me, and H), they are 0.951 (**11**), 0.743 (**12**), and 0.946 (**13**) for Group 2 (Y = NO_2, COOEt, Br, and Cl). The ratios in *a* (**13**)/*a* (**11**) are 0.254 and 0.995 for Group 1 and Group 2, respectively.

Panels a and b of Figure 8 show the plot of δ(Se: **14**)$_{SCS}$ versus δ(Se: **1**)$_{SCS:213}$ and δ(Se: **3**)$_{SCS:213}$, respectively. The δ(Se: **14**)$_{SCS}$ values for Y = H, Cl, and Br are very close to each other and that for Y = F is also close to them. The δ(Se: **14**)$_{SCS}$ value for Y = NO_2 is very different from that for Y = COOEt. The observations show the **pl** character of δ(Se: **14**)$_{SCS}$. Consequently, the structure is concluded to be **pl** for all members of **14**, although some equilibrium between **pl** and **pd** may contribute as the donor ability of Y becomes larger. The deviation of the data for Y = Me and OMe from the correlation line in Figure 8a must correspond to the equilibrium with **pd** for Y = Me and OMe.

δ(Se: **15**)$_{SCS}$ are reported not to correlate well with those of usual ArSeR such as δ(Se: **11**)$_{SCS}$.[3b] Panels a and b of Figure 9 show the plot of δ(Se: **15**)$_{SCS}$ versus δ(Se: **1**)$_{SCS}$ and δ(Se: **3**)$_{SCS}$, respectively. The correlation in Figure 9b is good (r^2 = 0.984). Therefore, the structure of **15** is concluded to be **pd** for all members in solutions, although a slight equilibrium with **pl** would contribute in solutions. The rules of thumb support this conclusion.

The plot of δ(Se: **16**)$_{SCS}$ versus δ(Se: $\mathbf{1_{pl}}$)$_{SCS}$ is of great interest, since the correlation constant is negative (a = −1.3). Further investigations are necessary to clarify the reason for the negative correlation, since the data for the plot are limited. δ(Se: **18**)$_{SCS}$ seem to correlate well with δ(Se: $\mathbf{1_{pl}}$)$_{SCS}$ and δ(Se: **17**)$_{SCS}$ are also expected to with δ(Se: $\mathbf{1_{pl}}$)$_{SCS}$. However, data for the plots are not enough to consider the structures in

solutions. δ(Se: **19**)$_{SCS}$ correlate well with δ(Se: **1** $_{pl}$)$_{SCS}$, which may show that **19** exists predominantly in **pl** in solutions, although data for the plot are not enough to conclude the structures, either.

The sp^2 and sp^3 carbon atoms are attached directly to the *p*-YC_6H_4Se group in **1** and **2**, respectively. Therefore, the correlation is expected to be better with δ(Se: **2**) than δ(Se: **1**) as the standard when δ(Se) from the π-framework in ArSeAr′ is examined and vice versa. This must be of great interest as the R effect in *p*-YC_6H_4SeR on δ(Se), although the observed magnitudes seem small.

Conclusion

A new set of δ(Se) are proposed for **pl**, employing 9-(arylselanyl)triptycenes (**1**: *p*-YC_6H_4SeTpc, Y = H (**a**), NMe_2 (**b**), OMe (**c**), Me (**d**), F (**e**), Cl (**f**), Br (**g**), COOEt (**h**), CN (**i**), and NO_2 (**j**)), in addition to the sets of δ(Se) proposed employing 9-(arylselanyl)anthracenes (**2** (**A**: **pl**)) and 1-(arylselanyl)anthraquionones (**3** (**A**: **pd**)). δ(Se: **2**) and δ(Se: **3**) must serve as the standard for **pl** and **pd** in solutions, respectively. The temperature dependence of δ(Se: **1**) is substantially improved relative to that for δ(Se: **2**). The character of δ(Se) in **1** (**pl**) is very similar to that in **2** (**pl**), although δ(Se: **1**) are different from δ(Se: **2**) for Y of halogens, which is of great interest. The character in **1** (**pl**) is very different from that of **3** (**pd**). δ(Se) of **1**−**3** are demonstrated to serve as the standard to determine the structures in solutions. Structures of various ArSeR for R of the benzene and naphthalene systems are determined in solutions from the viewpoint of the orientational effect based on δ(Se) of **1**−**3**. The rules of thumb derived from the characters in δ(Se) of **1** (**A**: **pl**), **2** (**A**: **pl**), and **3** (**A**: **pd**) are also very useful to determine the structures of ArSeR in solutions, in addition to the analysis of the plots.

Experimental Section

9-(Phenylselanyl)triptycene (1a). Under an argon atmosphere, to a solution of 9-bromotriptycene[21] (510 mg, 1.50 mmol) in 12 mL of benzene and 40 mL of diethyl ether at 0 °C was added 1.0 mL of *n*-BuLi (1.62 mmol, 1.62 M). After 1 h of stirring, the fine suspension of 9-triptycyllithum was added to an ethereal solution of 1.0 equiv of benzeneselenobromide. After being stirred for 1 h at 0 °C, the reaction was quenched by acetone (4 mL), and the solvent was removed in vacuo. A 100 mL sample of benzene and a 6% aqueous solution of hydrochloric acid were added. The organic layer was separated and washed with 50 mL of water, 50 mL of a 10% aqueous solution of sodium bicarbonate, 50 mL of a saturated aqueous solution of sodium hydrogen carbonate, and 50 mL of water and dried over anhydrous sodium sulfate. The crude product was purified by column chromatography (SiO_2, benzene/hexane 1:2 as eluent) and recrystallized from dichloromethane and hexane. **1a** was isolated in 32% yield as a colorless solid (195 mg): mp 271.0−272.5 °C; ^{1}H NMR (300 MHz, $CDCl_3$/TMS) δ 5.44 (s, 1H), 6.92 (dt, J = 1.4, 7.6 Hz, 3H), 7.01 (dt, J = 1.3, 7.4 Hz, 3H), 7.07−7.11 (m, 3H), 7.16−7.20 (m, 2H), 7.40 (dd, J = 1.2, 7.2 Hz, 3H), 7.54 (d, J = 7.4 Hz, 3H); ^{13}C NMR (75.5 MHz, $CDCl_3$/TMS) δ 54.2, 61.0, 123.3 (3C), 124.9 (^3J(Se,C) = 12.1 Hz, 3C), 125.0 (3C), 125.4, 125.8 (3C), 128.7 (*m*-Ph, 2C,), 129.9 (^2J(Se,C) = 15.6 Hz, 2C), 130.7, 144.0 (^2J(Se,C) = 6.2 Hz, 3C), 145.3 (3C); ^{77}Se (57.3 MHz, $CDCl_3$/Me_2Se) δ 259.0. Anal. Calcd for $C_{26}H_{18}Se$: C, 76.28; H, 4.43. Found: C, 76.42; H, 4.33.

9-[*p*-(*N*,*N*-Dimethylamino)phenylselanyl]triptycene (1b). Under a nitrogen atmosphere, to a suspension of di-9-triptycyl diselenide[22] (900 mg, 1.38 mmol) and 40 mL of THF at 0 °C was added $NaBH_4$ (110 mg, 2.76 mmol) in a small amount of water. A solution of 6.0 equiv of *p*-(*N*,*N*-dimethylamino)phenyldiazonium chloride was added at 0 °C. If an orange precipitate appeared, $NaBH_4$ (110 mg, 2.76 mmol) in an aqueous THF solution was added to the reaction solution. Dichloromethane (200 mL) and a 2% aqueous solution of sodium hydroxide were added. The organic layer was separated and washed with a 10% aqueous solution of sodium bicarbonate and a saturated aqueous solution of sodium hydrogen carbonate, then dried over potassium carbonate. The crude product was purified by column chromatography (SiO_2, benzene/hexane 1:1 as eluent) and recrystallization from hexane. **1b** was isolated in 6% yield as pale yellow needles (19 mg): mp 227.5−229.0 °C; ^{1}H NMR (300 MHz, $CDCl_3$/TMS) δ 2.87 (s, 6H), 5.42 (s, 1H), 6.55 (d, J = 9.0 Hz, 2H), 6.94 (dt, J = 1.5, 7.5 Hz, 3H), 7.01 (dt, J = 1.3, 7.3 Hz, 3H), 7.10 (d, J = 9.1 Hz, 2H), 7.40 (dd, J = 1.3 and 7.1 Hz, 3H), 7.60 (d, J = 7.4 Hz, 3H); ^{13}C NMR (75.5 MHz, $CDCl_3$/TMS) δ 40.5 (2C), 54.3, 60.5, 113.4 (2C), 123.1 (3C), 125.0 (3C), 125.1 (3C), 125.1, 125.6 (3C), 131.0 (^2J(Se,C) = 15.3 Hz, 2C), 144.5 (^2J(Se,C) = 6.2 Hz, 3C), 145.4 (3C), 148.6; ^{77}Se (57.3 MHz, $CDCl_3$/Me_2Se) δ 238.5. Anal. Calcd for $C_{28}H_{23}NSe$: C, 74.33; H, 5.12; N, 3.10. Found: C, 74.13; H, 5.11; N, 3.14.

The preparations of **1c**−**1j** are given in the SI.

QC Calculations. Quantum chemical (QC) calculations are performed on **1a** (Y = H) with use of the Gaussian 03 program[14] at the density functional theory (DFT) level of the Becke three-parameter hybrid functional combined with the Lee−Yang−Parr correlation functional (B3LYP)[15,16] and the Møller−Plesset second order energy correlation (MP2)[17] levels.

Acknowledgment. This work was partially supported by a Grant-in-Aid for Scientific Research (Nos. 16550038, 19550041, and 20550042) from the Ministry of Education, Culture, Sports, Science and Technology, Japan.

Supporting Information Available: Plots of $\delta(Se)_{SCS}$ in **11** (**11′**) versus δ(Se: **1**)$_{SCS:213}$ and/or δ(Se: **2**)$_{SCS:213}$, experimental procedure, preparations of **1c**−**1j**, NMR spectra of **1**, complete reference 14, and optimized structures given by Cartesian coordinates for **1a** at the DFT (B3LYP) and MP2 levels. This material is available free of charge via the Internet at http://pubs.acs.org.

JO801786J

(21) Bartlett, P. D.; Cohen, S. G.; Cotman, J. D., Jr.; Kornblum, N.; Landry, J. R.; Lewis, E. S. *J. Am. Chem. Soc.* **1950**, *72*, 1003–1004.

(22) Ishii, A.; Matsubayashi, S.; Takahashi, T.; Nakayama, J. *J. Org. Chem.* **1999**, *64*, 1084–1085.